

## Ultrasound liquid crystal lens

Yuki Shimizu,<sup>1</sup> Daisuke Koyama,<sup>1,a)</sup> Marina Fukui,<sup>1</sup> Akira Emoto,<sup>1</sup> Kentaro Nakamura,<sup>2</sup> and Mami Matsukawa<sup>1</sup>

<sup>1</sup>*Faculty of Science and Engineering, Doshisha University, 1-3 Tataramiyakodani, Kyotanabe, Kyoto 610-0321, Japan*

<sup>2</sup>*Laboratory for Future Interdisciplinary Research of Science and Technology, Tokyo Institute of Technology, 4259-R2-26, Nagatsuta-cho, Midori-ku, Yokohama 226-8503, Japan*

(Received 28 February 2018; accepted 8 April 2018; published online 19 April 2018)

A variable-focus lens using a combination of liquid crystals and ultrasound is discussed. The lens uses a technique based on ultrasound vibration to control the molecular orientation of the liquid crystal. The lens structure is simple, with no mechanical moving parts and no transparent electrodes, which is helpful for device downsizing; the structure consists of a liquid crystal layer sandwiched between two glass substrates with a piezoelectric ring. The tens-of-kHz ultrasonic resonance flexural vibration used to excite the lens generates an acoustic radiation force on the liquid crystal layer to induce changes in the molecular orientation of the liquid crystal. The orientations of the liquid crystal molecules and the optical characteristics of the lens were investigated under ultrasound excitation. Clear optical images were observed through the lens, and the focal point could be controlled using the input voltage to the piezoelectric ring to give the lens its variable-focus action. *Published by AIP Publishing.* <https://doi.org/10.1063/1.5027131>

In everyday life, various electric products can be found which use liquid crystals, such as cellular phones and personal computers. Scientific research into liquid crystals was triggered by the discovery of thermotropic liquid crystals by an Austrian botanist called Friedrich Reinitzer in the 19th century. Liquid crystals exist in an intermediate state between liquid and solid and have both liquid properties and crystalline material anisotropies because the liquid crystal molecules have directors. Anisotropic liquid crystal molecules have both electric and magnetic dipoles and can be classified as thermotropic or lyotropic based on the type of phase transition made from the liquid to the solid phase.<sup>1</sup> The molecules of thermotropic liquid crystals have elongated, disk-like,<sup>2</sup> or banana-like,<sup>3</sup> shapes and liquid crystals can be classified into three specific types (nematic, smectic, and cholesteric) based on their molecular aggregation state. Nematic liquid crystals have high liquidity and are widely used in industrial products such as liquid crystal displays because their molecular orientations can be controlled easily using an external field.<sup>4,5</sup> In general, transparent electrodes are required for liquid crystal devices to allow electric fields to be applied through the liquid crystal layer to control its molecular orientation. Indium tin oxide (ITO) is commonly used as a transparent electrode material because of its high transparency. However, ITO contains the rare metal indium, and ITO electrodes are generally fabricated by sputter deposition, which has both high equipment costs and complex processing requirements.<sup>6</sup> In addition, there is also a trade-off between low resistivity and high transparency in ITO.<sup>7,8</sup> Alternative transparent materials to replace ITO are currently under development and will enable realization of flexible liquid crystal devices such as electronic digital paper.<sup>9</sup>

The optical anisotropy of liquid crystals can be applied in a variety of optical devices. Sato and colleagues used the birefringence of liquid crystals to fabricate a variable-focus optical lens.<sup>10–14</sup> The refractive index of this lens can be changed by applying an electric voltage to the transparent electrodes, thus enabling control of the focal length. These liquid lenses, which contain no mechanical moving parts, are advantageous in terms of both robustness and downsizing of electronic modules because the camera modules in electronic devices such as cellular phones consist of a lens, an actuator, and a gearing system to move the lens in the axial direction and enable focal point sweeping. However, these micro-scale liquid crystal devices require complex patterning of the transparent ITO electrodes to accommodate the optical design.<sup>15</sup>

Ultrasound is a promising candidate technology that may help to solve the problems with transparent electrodes. Several researchers have reported the effects of application of ultrasound to nematic liquid crystals,<sup>16–18</sup> while ultrasound propagation in liquid crystals was also observed optically. The propagation of an ultrasound wave also means an instantaneous pressure change, which then induces a change in both the molecular orientation and the refractive index of the liquid crystal. Our group has therefore been investigating techniques for control of liquid crystal molecular orientations using ultrasound which require no transparent electrodes.<sup>19</sup> The crystal orientation direction can be changed statically using the acoustic radiation force. A two-dimensional periodic molecular orientation pattern can be induced by excitation of the resonance vibration mode of the glass substrate.<sup>20</sup> Switching of the resonance vibration mode allows the wavefront of the transmitted light to be controlled, and this technique can be applied to microlens arrays,<sup>21–23</sup> optical waveguides, and photonic crystals.<sup>24–26</sup> In this paper, an optical liquid crystal lens that uses

<sup>a)</sup> Author to whom correspondence should be addressed: dkoyama@mail.doshisha.ac.jp

ultrasound vibration to change the lens focal point is discussed as the first step in the application to an optical device.

An ultrasound liquid crystal variable-focus lens was fabricated as shown in Fig. 1. A nematic liquid crystal (RDP-85475, DIC, Japan; refractive index  $n_o$  at 589 nm: 1.525; birefringence  $\Delta n$  at 589 nm: 0.298; transition temperature of SN point:  $-10^\circ\text{C}$ ; NI point:  $123.7^\circ\text{C}$ ; and viscosity: 93.7 mPa·s) was used. An annular piezoelectric lead zirconate titanate (PZT) transducer (C-213, Fuji Ceramics, Japan; inner diameter: 20 mm; outer diameter: 30 mm; and thickness: 1 mm) that was polarized in the thickness direction was bonded to a transparent circular glass plate labelled (a) (diameter: 30 mm and thickness: 0.7 mm) using epoxy. A second circular glass plate labelled (b) (diameter: 15 mm and thickness: 0.7 mm) was bonded at the centre of the glass plate (a) using epoxy that contained 50- $\mu\text{m}$ -diameter silica microspheres to allow a liquid crystal layer to be formed between the two glass discs. After a nematic liquid crystal was injected into the gap via the capillary effect, the liquid crystal layer was sealed completely using epoxy. The liquid crystal molecules were then oriented perpendicular to the glass plates because of the chemical interaction between the liquid crystal molecules and the polyimide films (vertical alignment type, SE-5811, Nissan Chemical, Japan) that were formed on the glass plates without rubbing.

By exciting the transducer using a continuous sinusoidal electric signal at its resonance frequency, a flexural vibration mode was then generated on the liquid crystal lens entirely through the liquid crystal layer. The acoustic radiation force<sup>27,28</sup> that was caused by the ultrasound wave that radiated from the flexural vibration acted on the liquid crystal layer, thus allowing the collective orientation of the liquid crystal to be changed. Because the acoustic radiation force is a static force that is generated by differences in the acoustic energy densities of different media, it acts on the boundaries among the liquid crystal layer, the glass plates, and the surrounding air, not to an individual liquid crystal molecule directly. In the case of the ultrasound liquid crystal lens, most of the acoustic energy that is generated via the PZT transducer vibrations remains within the glass plates and the liquid crystal layer because it is reflected at the lens surface as a result of the large acoustic impedance difference between the glass and the air. This discontinuity in the acoustic energy density generates the acoustic radiation force that acts from the medium with higher energy density (i.e., the glass and the liquid crystal) towards the medium with lower energy density (i.e., the air) so that the lens surface and the liquid crystal layer are statically deformed toward air, and the molecular orientation of the liquid crystal layer is changed.

The light that was transmitted through the ultrasound liquid crystal lens was measured under crossed Nicol conditions to determine the optical characteristics of the lens. A polarizer and an analyser were arranged orthogonally, and the liquid crystal cell was then installed between them. A He-Ne laser beam ( $\lambda = 632.8\text{ nm}$ ) with a beam width of 2 mm was passed through the cell, and the transmitted light from the analyser was received using a photodetector (2051-FS, Newport) with a detector diameter of 0.9 mm. The distribution of the mechanical ultrasound vibrational amplitude over the upper surface of the circular glass plate (b) was measured using a laser Doppler vibrometer (NLV-2500, Polytec).

Several resonance frequencies were excited on the lens at more than 20 kHz. In this work, the axisymmetric flexural vibration mode in the thickness direction which has no nodal line and one nodal circle at 63.6 kHz in the relatively low ultrasound frequency range was used. The distributions of light transmitted through the lens were measured by simultaneously rotating the polarizer and analyser in the in-plane direction under crossed Nicol conditions to investigate both the birefringence distribution of the liquid crystal and the relationship between the molecular orientation of the liquid crystal and the vibration distributions of the glass plates. An area of  $5 \times 5\text{ mm}^2$  at the centre of the cell was observed via scanning of a laser beam with a measurement pitch of 0.25 mm; both of the laser and the photodetector were moved simultaneously. In the case without ultrasound excitation, the transmitted light was filtered under crossed Nicol conditions because the liquid crystal molecules were oriented perpendicularly relative to the glass plates in the default condition [Fig. 2(a)]. When the input voltage was applied, a flexural vibration was generated on the lens and the transmitted light intensity distribution changed dramatically with changes in the polarization direction of the incident light  $\theta$  [Figs. 2(b) and 2(c)]. If the orientation direction of liquid crystal molecules is uniform in the thickness direction, the light intensity distribution should correspond at  $\theta = 0^\circ$  [Fig. 2(b)] and  $90^\circ$  [Fig. 2(c)] under the crossed Nicol conditions because the transmitted light intensity can be expressed as a function of  $\sin^2 2\theta$ . The maximum light intensity is observed at  $\theta = 45^\circ$  and  $135^\circ$  since the transmitted light is polarized elliptically through the liquid crystal layer. Therefore, these experimental results mean that the liquid crystal molecules were twisted in the thickness direction. When we focus on one observation point changing the polarization direction  $\theta$ , the maximum light intensity was obtained for the case where the polarization direction of transmitted light through the cell corresponded to the orientation direction of the analyser. Under this hypothesis, we can assume that the orientation direction at the upper surface of the liquid crystal layer

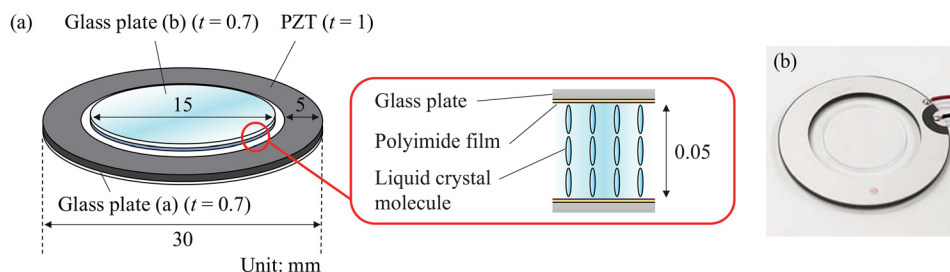


FIG. 1. (a) Configuration and (b) photograph of the ultrasonic liquid crystal lens.

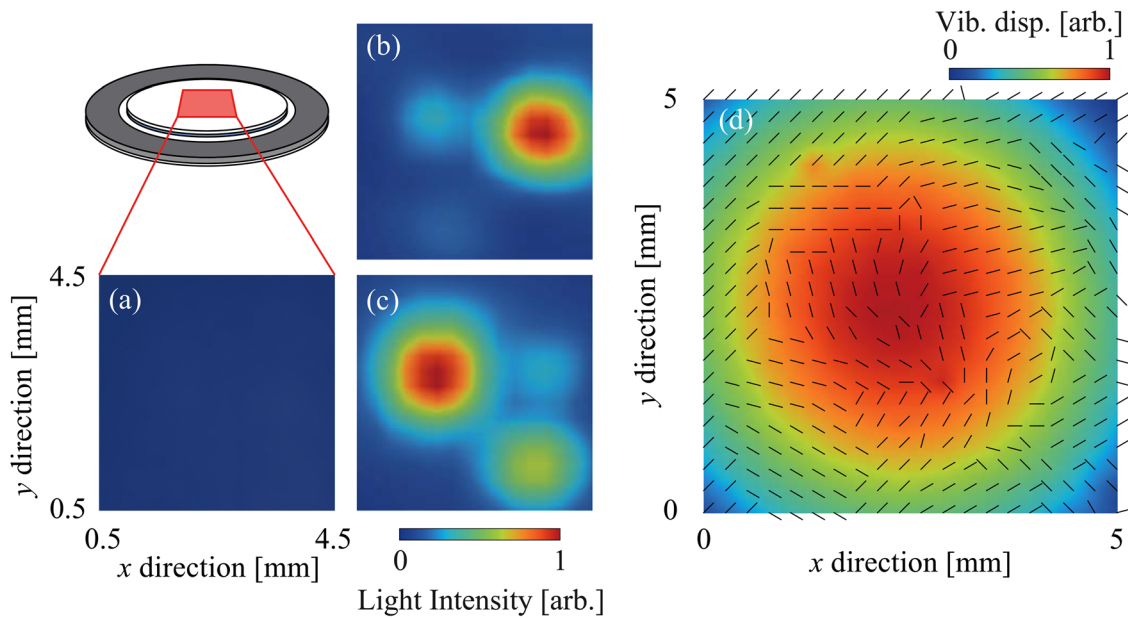


FIG. 2. Distributions of the transmitted light intensity (a) without ultrasound excitation and with ultrasound excitation at polarization directions ( $\theta$ ) of (b)  $0^\circ$  and (c)  $90^\circ$ . (d) Distributions of the vibrational amplitude of the glass substrate and the orientation directions of the liquid crystal molecules at 63.6 kHz.

corresponds to the same direction since the polarization direction of transmitted light is strongly affected by the molecular orientation at the upper surface.<sup>20</sup> Figure 2(d) shows the distributions of both the vibrational amplitude and the liquid crystal molecular orientation at the upper surface which occurred under ultrasound excitation at 63.6 kHz. The distributions of the vibrational displacement amplitude and the orientation were expressed using a colour scale and bars, respectively, and the vibrational amplitude was normalized with respect to the maximum value (where the maximum vibrational displacement amplitude was  $0.47 \mu\text{m}$  when the electric power consumption was 2 mW). The distributions of the orientation direction were obtained by measuring the polarization direction of the incident light  $\theta$  which gives the maximum light intensity of the transmitted light at each measurement point. The molecular orientations flowed outward from the loop positions, and these two distributions were correlated, thus indicating that the change in the molecular orientation in the liquid crystal layer was caused by the acoustic radiation force that was generated by the flexural vibrations of the glass plate. Strictly speaking, the acoustic radiation force distribution is directly dependent on the acoustic field in the liquid crystal layer because the acoustic radiation force can be expressed as a function of the square of the sound pressure amplitude, and the acoustic field will be similar to a Bessel function, which is the theoretical solution for a disk cavity.<sup>29</sup> The result shown in Fig. 2(d) indicates that the liquid crystal molecules were twisted asymmetrically in the thickness direction although the configuration of the lens was symmetrical in the thickness direction (the liquid crystal layer was sandwiched between two glass plates with the same thickness). This asymmetric twisting orientation is attributed to impedance mismatching between glass plates (a) and (b) and attenuation of the ultrasound in the liquid crystal layer. In fact, the ratio of the vibrational amplitude of glass plate (b) to that of glass plate (a) was 0.97. In addition, in the cases of the cell with different liquid crystal layer

thicknesses, the distribution of the molecular orientation in the liquid crystal layer varied because the anchoring strength of the liquid crystal layer to the orientational polyimide film increased as the liquid layer thickness decreased.<sup>30</sup>

The optical image that passed through the ultrasound liquid crystal lens was observed using a transmission optical microscope (VW-9000, Keyence) with an objective lens ( $\times 200$ ) under the condition that one Nicol element was used to evaluate the optical characteristics of the lens simply in one polarization direction (see Fig. 3). A resolution test target (1951 USAF) was positioned parallel to the lens between the light source and a polarizer at a distance of 22 mm from the lens surface. Figure 3 shows representative captured images of the test target without and with applied excitation which indicate that the focal position was changed by the ultrasound vibration. The focal length was evaluated quantitatively by moving the test target along the optical axis

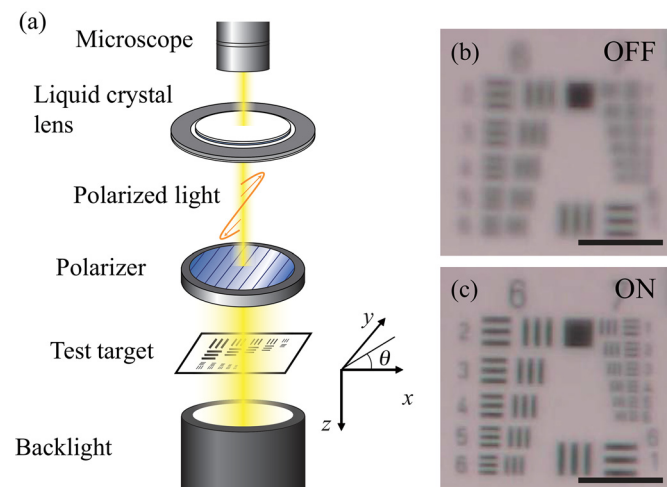


FIG. 3. (a) Observation setup and images captured using a microscope through the liquid crystal lens (b) without and (c) with ultrasound excitation. The bars in the images indicate  $100 \mu\text{m}$ .



(in the  $z$  direction) between the polarizer and the optical source. The focal position was determined based on the sharpness of the captured image and calculated using a spatial derivative. Figure 4 shows the relationship between the electric power consumption of the PZT transducer and the focal length of the liquid crystal lens. Because the total optical characteristics are dependent on the optical system using the microscope, the focal length of the lens without applied ultrasound excitation was determined to be 0 mm, while a negative value for the focal length indicates that the focal point approaches the lens surface from the negative  $z$  direction. As the electric power to the lens increased from 0 to 6.6 mW (the input voltage of 2.3 V<sub>rms</sub>), the focal length gradually decreased and the focal point approached the lens surface. The liquid crystal lens thus acted as a convex lens under ultrasound excitation, and higher electric power would give a smaller radius of curvature because the acoustic radiation force that was transmitted to the liquid crystal layer increased with increasing electric power. The focal length did not depend on the polarization direction of the incident light since the configuration of the lens and the orientation directions of the liquid crystal molecules were axisymmetric as shown in Fig. 2(d). In this electric power consumption range, the ultrasonic vibration on the lens has little effect on the captured image because the vibrational amplitude is relatively small (approximately 1  $\mu$ m). The electric power consumption of the ultrasound liquid crystal lens will be larger than that of a liquid crystal tunable lens using ITO electrodes (tens of  $\mu$ W) although the input voltage to the ultrasound lens was equal to or smaller.<sup>10,31</sup> This is because the ultrasound liquid crystal lens utilizes the resonance condition where the electric impedance decreases and the input current increases dramatically. The focal point could be controlled

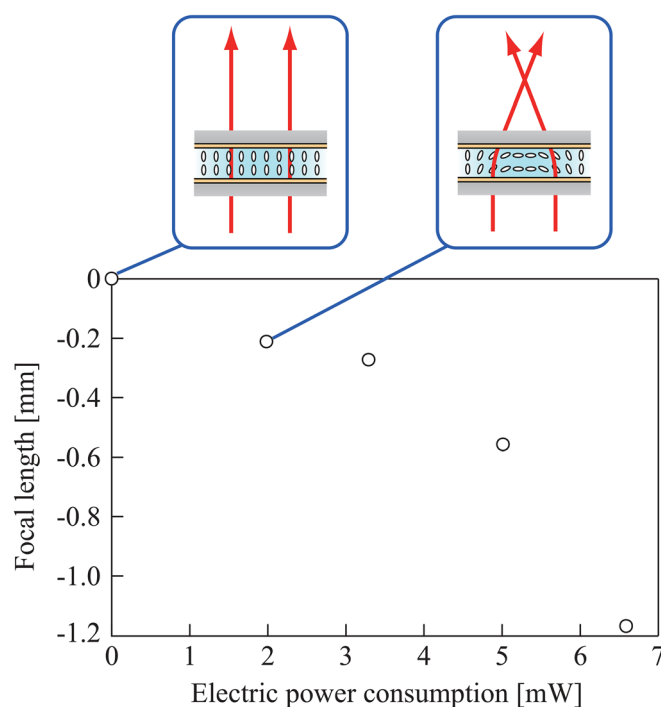


FIG. 4. Schematics showing changes in the molecular orientation of the liquid crystal and the relationship between electric power consumption and the focal length of the lens.

using the input voltage, and the lens thus acted as a variable-focus lens. This phenomenon can be explained based on the results shown in Fig. 2; the molecular orientation of the liquid crystal gradually inclines towards the centre of the lens in the thickness direction, and the incident light was then refracted along the molecular orientation and focused through the liquid crystal layer. Apparently, the lens profiles are determined uniquely by each input voltage because the lens uses the resonance vibration modes, and the acoustic resonance fields are generated within the liquid crystal layer. However, compensation of the optical aberrations and control of the focal point in the radial direction can be achieved through the use of the divided electrodes and control of the input voltages.<sup>32</sup>

In summary, an ultrasound liquid crystal lens was proposed. This lens has a simple structure that is helpful for device downsizing, and it can be installed directly on electronic substrates. The lens used a technique based on ultrasound vibration to control the molecular orientation of the liquid crystal. The optical characteristics of the lens could be controlled using the input voltage and allowed it to act as a variable-focus lens.

This work was partly supported by a KAKENHI Grant-in-Aid (No. 16K14204) from the Japan Society for the Promotion of Science (JSPS) and by research grants from the Kurata Memorial Hitachi Science and Technology Foundation, the Konica Minolta Science and Technology Foundation, the Takano Science Foundation, and the Kyoto Technoscience Center. We thank David MacDonald, MSc, from the Edanz Group ([www.edanzediting.com/ac](http://www.edanzediting.com/ac)) for editing a draft of this manuscript.

- <sup>1</sup>M. J. Stephen and J. P. Straley, *Rev. Mod. Phys.* **46**, 617 (1974).
- <sup>2</sup>S. K. Pal, S. Setia, B. S. Avinash, and S. Kumar, *Liq. Cryst.* **40**, 1769 (2013).
- <sup>3</sup>L. A. Madsen, T. J. Dingemans, M. Nakata, and E. T. Samulski, *Phys. Rev. Lett.* **92**, 145505 (2004).
- <sup>4</sup>M. Schadt and W. Helfrich, *Appl. Phys. Lett.* **18**, 127 (1971).
- <sup>5</sup>M. F. Schiekel and K. Fahrenshon, *Appl. Phys. Lett.* **19**, 391 (1971).
- <sup>6</sup>K. Azuma, K. Sakajiri, H. Matsumoto, S. Kang, J. Watanabe, and M. Tokita, *Mater. Lett.* **115**, 187 (2014).
- <sup>7</sup>P. Perkowski, *Opto-Electron. Rev.* **17**, 180 (2009).
- <sup>8</sup>H. Kawazoe, M. Yasukawa, H. Hyodo, M. Kurita, H. Yanagi, and H. Hosono, *Nature* **389**, 939 (1997).
- <sup>9</sup>M. Vosgurtichian, D. J. Lipomi, and Z. Bao, *Adv. Funct. Mater.* **22**, 421 (2012).
- <sup>10</sup>S. Sato, *Jpn. J. Appl. Phys., Part 1* **18**, 1679 (1979).
- <sup>11</sup>T. Nose and S. Sato, *Liq. Cryst.* **5**, 1425 (1989).
- <sup>12</sup>T. Nose, S. Masuda, and S. Sato, *Jpn. J. Appl. Phys., Part 2* **30**, L2110 (1991).
- <sup>13</sup>M. Ye, Y. Yokoyama, and S. Sato, *Appl. Phys. Lett.* **89**, 141112 (2006).
- <sup>14</sup>M. Ye, B. Wang, and S. Sato, *IEEE Photonics Technol. Lett.* **18**, 505 (2006).
- <sup>15</sup>M. Kawamura, K. Nakamura, and S. Sato, *Opt. Express* **21**, 26520 (2013).
- <sup>16</sup>H. Mailar, K. L. Likins, T. R. Taylor, and J. L. Ferguson, *Appl. Phys. Lett.* **18**, 105 (1971).
- <sup>17</sup>W. Helfrich, *Phys. Rev. Lett.* **29**, 1583 (1972).
- <sup>18</sup>S. Naga and K. Iizuka, *Jpn. J. Appl. Phys., Part 1* **13**, 189 (1974).
- <sup>19</sup>S. Taniguchi, D. Koyama, Y. Shimizu, A. Emoto, K. Nakamura, and M. Matsukawa, *Appl. Phys. Lett.* **108**, 101103 (2016).
- <sup>20</sup>Y. Shimizu, D. Koyama, S. Taniguchi, A. Emoto, K. Nakamura, and M. Matsukawa, *Appl. Phys. Lett.* **111**, 231101 (2017).
- <sup>21</sup>M. Reznikov, Y. Reznikov, K. Slyusarenko, J. Varshal, and M. Manevich, *J. Appl. Phys.* **111**, 103118 (2012).
- <sup>22</sup>M. Xu, Z. Zhou, H. Ren, S. H. Lee, and Q. Wang, *J. Appl. Phys.* **113**, 053105 (2013).
- <sup>23</sup>J. Kim, J. Kim, J. Na, B. Lee, and S. Lee, *Opt. Express* **22**, 3316 (2014).

- <sup>24</sup>R. Ozaki, T. Matsui, M. Ozaki, and K. Yoshino, [Appl. Phys. Lett.](#) **82**, 3593 (2003).
- <sup>25</sup>R. Ozaki, M. Ozaki, and K. Yoshino, [Jpn. J. Appl. Phys., Part 2](#) **43**, L1477 (2004).
- <sup>26</sup>R. Ozaki, H. Moritake, K. Yoshino, and A. A. Zakhidov, [Mol. Cryst. Liq. Cryst.](#) **545**, 67–1291 (2011).
- <sup>27</sup>B. Chu and E. Apfel, [J. Acoust. Soc. Am.](#) **72**, 1673 (1982).
- <sup>28</sup>D. Koyama, R. Isago, and K. Nakamura, [Appl. Phys. Lett.](#) **100**, 091102 (2012).
- <sup>29</sup>J. W. S. Rayleigh, *The Theory of Sound* (Dover, New York, 1945), Vol. 2, p. 297.
- <sup>30</sup>C. Y. Huang, Y. S. Huang, and J. R. Tian, [Jpn. J. Appl. Phys., Part 1](#) **45**, 168 (2006).
- <sup>31</sup>A. F. Naumov, M. Y. Loktev, I. R. Guralnik, and G. Vdovin, [Opt. Lett.](#) **23**, 992 (1998).
- <sup>32</sup>D. Koyama, R. Isago, and K. Nakamura, [IEEE Trans. Ultrason., Ferroelectr., Freq. Control](#) **58**, 2720 (2011).